Supplementary materials for

Temperature-induced densification in compressed basaltic glass revealed by in-situ ultrasonic measurements

Man Xu[1,2], Zhicheng Jing[3*], Young Jay Ryu[1], Julien Chantel[4], James A. Van Orman[2], Tony Yu[1], Yanbin Wang[1]

[1]Center for Advanced Radiation Sources, The University of Chicago, Chicago, IL 60637, USA

[2]Department of Earth, Environmental, and Planetary Sciences, Case Western Reserve University, Cleveland, OH 44106, USA

[3]Department of Earth and Space Sciences, Southern University of Science and Technology, Shenzhen, Guangdong, 518055, China

[4]University of Lille, CNRS, INRAE, Centrale Lille, UMR 8207 - UMET - Unité Matériaux et Transformations, 59000 Lille, France

[*]Correspondence to: Z. Jing, jingzc@sustech.edu.cn

Uncertainty analysis

Here we present detailed analysis of the uncertainty of the determined acoustic velocity. Uncertainty in the determined travel time through the pulse-echo overlap method (Kono et al. 2012; Li and Liebermann 2014; Jing et al. 2020) is generally small, and is estimated to be within ±0.2 ns for all experiments reported in this study, which corresponds to a relative uncertainty of ~0.1% in the velocity. The major uncertainty comes from the sample length determination through X-ray radiographic imaging. Flat and parallel sample interfaces are necessary for accurately determining the sample length. In this study, all velocity data reported were measured on samples that relatively flat interfaces were maintained at high P-T conditions during the experiments. To estimate the

uncertainty from sample length measurements, we have carefully analyzed the profile of image gray value derivative vs. pixel distance for each sample image. Ideally, the sharp contrast between sample and Mo capsule should display a very sharp peak in the profile with the peak position corresponds to the pixel position of the sample interface. However, an uneven or tilted interface can result in broadening of the peak. We thus choose to use the peak width to estimate the uncertainty in sample length determination. Each peak was fitted with a gaussian function in the form of $y_0 + Aexp\left[-\left(\frac{x-x_0}{width}\right)^2\right]$, where x_0 gives the pixel position for the sample interface and half width gives the uncertainty of the position. The uncertainties of the top and bottom sample interfaces were then propagated according to standard error propagation. The total uncertainty in sample length are smaller than 3 pixels for all the sample images collected (1 pixel = 1.77 μm), translating to a relative uncertainty of ~0.7% in the acoustic velocity.

Calculation of velocity reduction using glass and melt results in Fig. 6b

The velocity anomaly due to the presence of partial melts was evaluated using both the glass and melt velocity behaviors in Fig. 6b. The equation of state of model basalt liquid from (Asimow and Ahrens 2010) was used to calculate the aggregate velocity of a simplified partial melt system (PREM (Dziewonski and Anderson 1981) + various fractions of model basalt melt, where PREM is used to represent the solid mantle). The negative pressure dependence of velocities in cold-compressed model basalt glass below ~8 GPa was also used to model the partial melt velocities for comparison. The measured glass velocities are unrelaxed and cannot be directly compared with seismic wave velocities, so an anchor point of room-pressure melt velocity was used and combined with the pressure dependence of velocity determined for the model basalt glass in this study to model melt velocities at high pressures, which is similar to the approach used in (Clark et al. 2016;

Clark and Lesher 2017). A simple additive model (the Voigt limit) is employed to calculate the aggregate velocity as a function of pressure and melt fraction. Although the exact melt fraction needed for a given velocity reduction cannot be determined by this simple additive model as the velocity of partially molten assemblage also depends on realistic melt geometries (Takei 2002), the simple model can still provide instructive information on the relative effect of pressure and melt fraction on the velocity reduction due to partial melts.

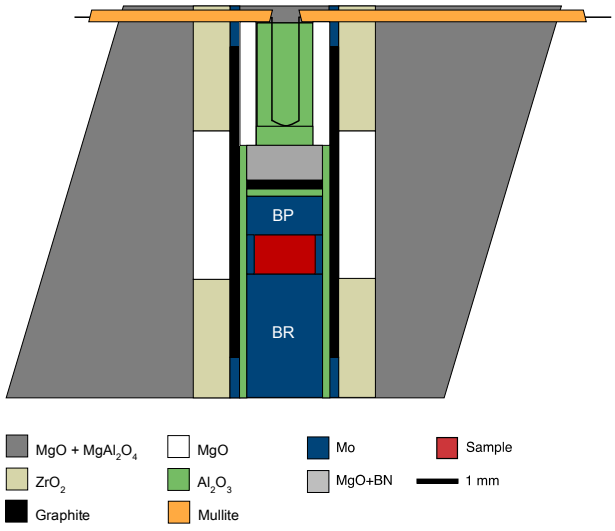

Fig. S1 Experimental cell assembly used for ultrasonic measurements. BR-buffer rod, BP-backing plate.

Table S1 Experimental conditions and results of acoustic velocity measurements on model basalt glass along different P-T paths.

Experimental type	Run#	Comments	Load (ton)	P (GPa)	T (K)	V_P (m/s)	V_S (m/s)
Cold compression	T2545	Compression	25	0.60	300	6324	3508
			50	0.70	300	6292	3489
			75	1.10	300	6283	3452
			100	2.45	300	6219	3386
			125	3.50	300	6108	3295
			150	4.29	300	6047	3268
			175	5.87	300	6013	3223
			200	6.73	300	5960	3181
			225	7.58	300	5859	3120
			250	8.22	300	5842	3112
Cold compression	T2743	Compression	25	0.82	300	6326	3497
			50	1.59	300	6235	3436
			75	2.39	300	6170	3412
			100	2.82	300	6153	3392
			125	3.78	300	6112	3363
			150	5.00	300	6021	3316

			175	6.44	300	5961	3251
			200	6.94	300	5932	3221
			225	7.89	300	5883	3192
			250	8.49	300	5971	3229
			275	9.37	300	6057	3260
			300	9.95	300	6176	3298
			325	10.22	300	6298	3341
			350	10.74	300	6470	3402
			375	11.46	300	6577	3436
			400	11.74	300	6712	3491
			430	12.24	300	6819	3538
		Decompression	350	11.68	300	6909	3603
			280	11.14	300	6964	3646
			210	9.76	300	6918	3654
			150	8.23	300	6874	3691
			100	5.69	300	6730	3698
			80	4.98	300	6647	3694
			60	3.45	300	6537	3690
			40	1.84	300	6494	3688
			20	0.95	300	6438	3716
Hot compression	T2689	Compression	20	0.32	641	6430	3585

	40	1.01	641	6404	3532
	60	1.81	641	6319	3468
	80	2.60	641	6285	3443
	100	3.10	641	6256	3398
	120	3.73	641	6211	3370
	140	4.56	641	6166	3324
	160	5.39	641	6129	3297
	180	6.21	641	6166	3291
	200	6.84	641	6227	3316
	220	7.18	641	6322	3366
	240	8.33	641	6508	3448
	260	8.64	641	6627	3501
	280	8.84	641	6703	3517
Decompression	250	8.46	641	6805	3573
	200	7.63	641	6833	3602
	150	6.82	641	6814	3619
	125	6.45	641	6795	3634
	100	5.71	641	6756	3640
	80	4.74	641	6714	3635
	60	3.80	641	6653	3631
	50	3.38	641	6617	3635
	40	2.69	641	6578	3636
	25	1.47	641	6487	3613

			15	0.71	641	6452	3626
Hot compression	T2690	Compression	20	0.83	823	6488	3608
			40	1.19	823	6464	3551
			60	1.53	823	6444	3538
			80	2.27	823	6462	3528
			120	3.01	823	6503	3523
			140	3.64	823	6519	3519
			160	4.53	823	6556	3528
			180	5.37	823	6614	3543
			200	5.74	823	6699	3571
			220	5.93	823	6722	3580
			240	6.69	823	6832	3617
			260	7.05	823	6895	3628
			280	7.75	823	6964	3662
			300	7.91	823	7023	3692
		Decompression	250	7.26	823	7077	3735
			200	6.70	823	7073	3753
			150	6.01	823	7044	3763
			100	4.92	823	6969	3768
			75	3.79	823	6904	3763
			50	3.08	823	6809	3750

			25	1.59	823	6681	3732
			15	1.13	823	6609	3706
Hot compression	T2698	Compression	30	0.90	1006	6414	3500
			60	1.65	1006	6431	3511
			80	2.41	1006	6469	3515
			100	3.16	1006	6546	3525
			120	3.75	1006	6632	3540
			140	4.45	1006	6651	3557
			160	5.08	1006	6690	3558
			180	5.74	1006	6726	3564
			200	6.59	1006	6808	3581
			220	7.02	1006	6877	3618
			240	7.49	1006	6950	3632
			260	7.67	1006	6989	3646
			280	7.98	1006	7019	3652
			300	8.27	1006	7060	3664
		Decompression	250	8.05	1006	7094	3695
			200	7.38	1006	7090	3705
			150	6.76	1006	7062	3716
			100	5.54	1006	6985	3729
			60	4.27	1006	6863	3705

			20	2.24	1006	6626	3632
Heating-cooling at fixed load	T2364	Heating	100	2.74	300	6553	3528
			100	2.60	458	6520	3498
			100	2.15	641	6515	3494
		Cooling	100	2.23	823	6572	3514
			100	1.73	641	6591	3550
			100	1.51	458	6621	3576
			100	1.24	300	6647	3616
		Heating	150	4.15	300	6649	3590
			150	4.32	458	6620	3573
			150	4.29	641	6564	3508
		Cooling	150	3.91	823	6584	3542
			150	3.88	641	6737	3586
			150	3.65	458	6783	3643
			150	3.22	300	6811	3677
		Heating	200	5.34	300	6840	3644
			200	5.66	458	6819	3608
			200	6.06	641	6759	3559
		Cooling	200	5.68	823	6814	3567
			200	5.41	641	6863	3638

		200	5.15	458	6915	3679
		200	4.97	300	6950	3712
	Heating	250	6.73	300	7010	3693
		250	7.07	458	6973	3672
		250	7.43	549	6942	3643
		250	7.47	641	6924	3615
	Cooling	250	7.11	823	7066	3633
		250	6.83	641	7092	3720
		250	6.46	458	7134	3751
		250	6.23	300	7167	3781

Note: Uncertainty in measured velocity is about 0.8%. Uncertainties in pressure and temperature are about 10% and 10 K, respectively.